

Effect of local joint flexibility on the fatigue life assessment of jacket-type offshore platform

Behrouz Asgarian^{*}, Parviz Kuzehgār^a and Pooya Rezadoost^b

Faculty of Civil Engineering, K.N. Toosi University of Technology, Tehran, Iran

(Received October 23 2023, Revised December 15, 2023, Accepted December 18, 2023)

Abstract. This paper investigates the impact of local joint flexibility (LJF) on the fatigue life of jacket-type offshore platforms. Four sample platforms with varying geometric properties are modeled and analyzed using the Opensees software. The analysis considers the LJF of tubular joints through the equivalent element and flexible link approaches, and the results are compared to rigid modeling. Initially, modal analysis is conducted to examine the influence of LJF on the frequency content of the structure. Subsequently, fatigue analysis is performed to evaluate the fatigue life of the joints. The comparison of fatigue life reveals that incorporating LJF leads to reduced fatigue damage and a significant increase in the longevity of the joints in the studied platforms. Moreover, as the platform height increases, the effect of LJF on fatigue damage becomes more pronounced. In conclusion, considering LJF in fatigue analysis provides more accurate results compared to conventional methods. Therefore, it is essential to incorporate the effects of LJF in the analysis and design of offshore jacket platforms to ensure their structural integrity and longevity.

Keywords: fatigue damage; local joint flexibility; modal analysis; offshore jacket platform; spectral fatigue analysis

1. Introduction

Jacket-type offshore platforms are steel space-braced frames composed of welded tubular members, commonly used in the offshore industry as the oil/gas platforms and substructure of offshore wind turbines (Nassiraei and Rezadoost 2022). The post-service analyses for jacket-type offshore platforms include in-place (Abdel Raheem *et al.* 2022), earthquake (Xu *et al.* 2023), fatigue (Han *et al.* 2022), and boat impact (Ladeira *et al.* 2022) analysis. Performing fatigue analysis is critically important in jacket-type offshore platforms because it can impact various factors, including the size of the chord (diameter and thickness of the chord, as well as the thickness and length of the can), brace size (diameter and thickness of the brace, as well as the thickness and length of the stub), welding method (single or double side welding), necessary inspection plan, and material selection. Fatigue in tubular joints is more critical than in tubular members for the following reasons:

^{*}Corresponding author, Professor, E-mail: asgarian@kntu.ac.ir

^aMaster, E-mail: kuzehgār.parviz@gmail.com

^bPh.D. Student, E-mail: p.rezadoost@email.kntu.ac.ir

1. A tubular joint is formed by welding a tube (brace) to the external surface of another tube (chord). Full penetration groove welding is employed to produce these joints which results in a Heat Affected Zone (HAZ) around the weld that is weakened and brittle.
2. Changes in the diameter and thickness of members at the joint result in stress concentration.
3. Due to the repeated loads acting on the platform, the joints in the structure are subjected to the highest forces, resulting in a high-stress range in these locations.

The analysis of jacket-type offshore platforms is typically conducted by assuming that the joints are rigid and that member end forces have no effect on chord wall deformations. However, in reality, the chord wall at the joint locally deforms under brace member end loads. Including joint local deformations in the analysis process can lead to increased deformations, changes in frequency content, and a redistribution of forces in the structure (Gao *et al.* 2013). Considering local joint flexibility (LJF) in the damage assessment of platforms leads to more realistic and precise results, ultimately improving the safety, reliability, and cost-effectiveness of structural design and maintenance. It is an essential aspect of modern engineering practice that considers real-world behavior for better decision-making. Overall, fatigue analysis considering LJF plays a significant role in the structural health assessment of existing platforms. It provides a more comprehensive understanding of how fatigue damage accumulates in joints and assists in optimizing inspection strategies to ensure the ongoing safe and efficient operation of the platform.

The primary objective of this paper is to investigate the influence of LJF on the fatigue life of tubular joints. Additionally, the paper aims to explore different methodologies for incorporating LJF into the analysis process, and subsequently conduct a comparative analysis among these approaches. To accomplish this, the study employed the OpenSees software to model and analyze four jacket platforms with varying geometric properties. The findings of the study compared the dynamic behavior of the structures, fatigue failure, and the required occurrence rates for inducing failure in tubular joints, considering both flexible and rigid joint modeling scenarios. The results obtained provide valuable insights into the importance of LJF in accurately predicting the dynamic response and fatigue life of tubular joints in the investigated platforms.

2. Literature survey

Mirtaheri *et al.* (2009) concluded that LJF has a noticeable effect on changing the static and dynamic behavior of the platform. They showed that the platform with flexible joints has more displacement and less base shear. Asgarian *et al.* (2015) described that structural analysis considering LJF has a better match with the result of the analyses on sophisticated 3D models of tubular members. The significant influence of LJF on structural behavior has led to the proposal of various parametric equations for calculating the LJF of different types of joints, including uni-planar gapped K-joints (Khan *et al.* 2018), three-planar tubular T-joints (Ahmadi and Akhtegan 2022), three-planar tubular Y-joints (Ahmadi and Niri 2023), and multi-planar tubular TT-joints (Ahmadi and Janfeshan 2021), among others.

Following the calculation of LJF, researchers have directed their attention toward exploring how to incorporate it into the analysis process. LJF can be taken into account in finite element models that utilize shell and solid elements, but modeling all members and joints of the platform within the finite element method would be excessively time-consuming. In their studies, Ren *et al.* (2021) and Ren *et al.* (2023) have suggested the application of super-element techniques as a means to enhance the precision of tubular joint representation in jacket-type platforms. Zhu *et al.* (2022) presented a

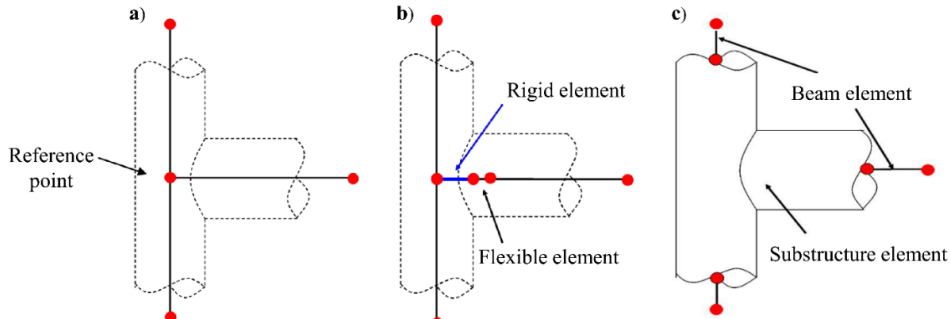


Fig. 1 Local Joint Flexibility modeling approaches. (a) Rigid link approach, (b) Equivalent element approach, and (c) Flexible link approach

simplified bar-system model that is both accurate and efficient for analyzing both nonlinear static problems and linear vibration problems. This model aims explicitly to simulate the LJF of tubular joints in a tubular structure. Golafshani *et al.* (2013) proposed a new element that considers the flexibility of joints without requiring prior knowledge of joint behavior. This element was developed by assuming that joint flexibility causes negligible axial deformation of the chord. Alanjari *et al.* (2011) proposed a 2D elastic-perfectly plastic tubular joint element based on flexibility equations and the interaction between axial force and in-plane bending moment. They concluded that joint modeling without LJF is unable to predict the structure's real lateral elastic stiffness accurately.

Previous studies have shown that LJF can significantly affect a structure's response, but the influence on joint fatigue life remains unclear. Moreover, several methods have been proposed for simulating LJF, and it is uncertain which approach yields the most realistic results for fatigue analysis.

3. Methodology

3.1 Local joint flexibility modeling approaches

This paper utilizes three ideas to model tubular joints and examine the effect of LJF on joints' fatigue life:

1. Rigid link approach (Fig. 1(a)): In this approach, members are rigidly connected to a reference point at the joint. This method does not consider shell behavior and the local deformation to the member's wall, but it is possible to obtain stresses in chord walls by applying a rigid element.
2. Equivalent element approach (Fig. 1(b)): In this approach, the values of the cross-sectional area, moment of inertia, and length of the element are determined in a way that the resulting flexibility matches that given by Buitrago *et al.*'s (1993) equations.
3. Flexible link approach (Fig. 1(c)): In the third approach, the link element developed by Alanjari *et al.* (2011), implemented in OpenSees software, is used. In this method, the concept of sub-structuring is used in modeling the LJF, and the joint's geometry is directly entered into the stiffness matrix.

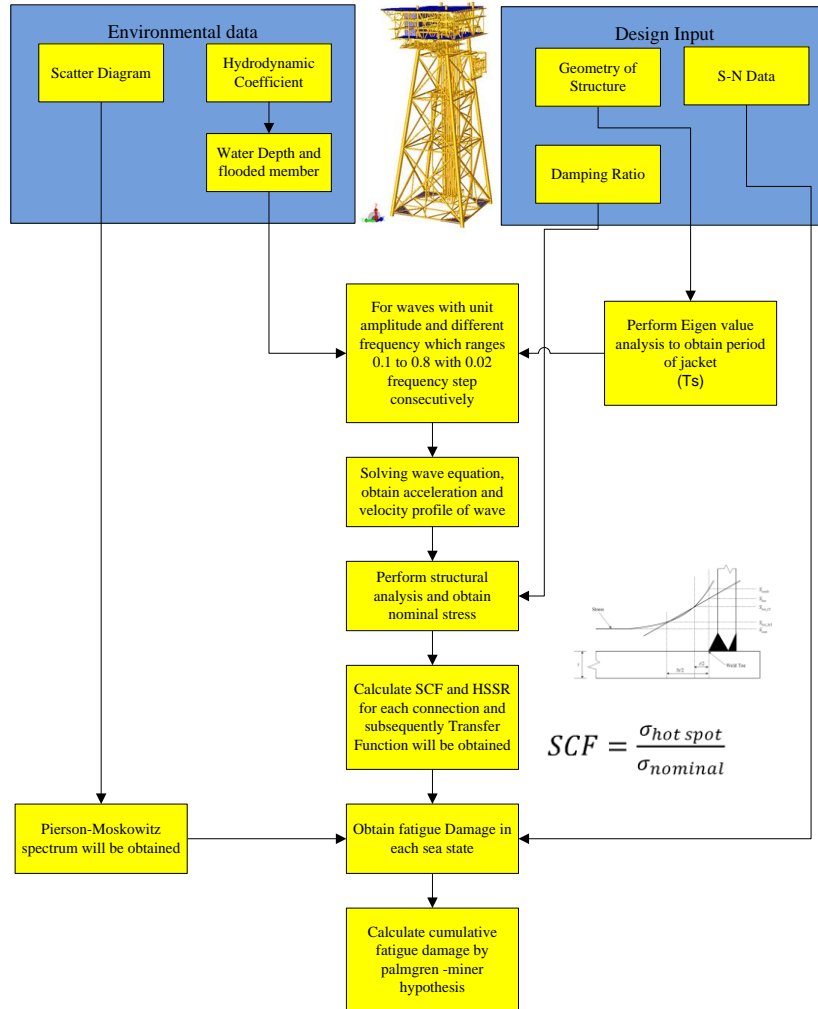


Fig. 2 Damage calculation procedure through spectral-based fatigue analysis

3.2 Fatigue damage

Fatigue analysis in offshore platforms is performed using deterministic and spectral methods. In deterministic fatigue analysis, for considering the dynamic nature of loads, only stresses are amplified by considering the dynamic amplification factor (DAF). However, the dynamic response of the platform is considered in the spectral fatigue analysis. The analysis procedure shown in Fig. 2 provides a comprehensive framework for conducting dynamic spectral fatigue analysis in offshore platforms. By using this approach, it is possible to accurately reflect the actual behavior of the platform and the sea states in the analysis.

In spectral fatigue analysis, waves are modeled as a set of sea states in the wave scatter diagram. Instead of applying each sea state with a significant wave height and period to the platform, the spectrum of that sea state is applied. In Table 1, a scatter diagram for the wave is presented.

Table 1 Sea state scatter diagram

Number of wave condition	Significant wave period (Ts)	Significant wave height (Hs)
1, 2, 3	1.5	0.25, 0.75, 1.25
4, 5, 6	2.5	0.25, 0.75, 1.25
7, 8, 9	3.5	0.25, 0.75, 1.25
10, 11, 12	4.5	0.25, 0.75, 1.25
13, 14, 15	5.5	0.75, 1.25, 1.75
16, 17, 18	6.5	1.25, 1.75, 2.25

One of the most popular spectrums that represent the random nature of waves is the Pierson-Moskowitz (PM) spectrum. This spectrum can be used for fully developed wave conditions where the fetch and the duration are large, and there is no disturbance from other areas. The Bretschneider's form of Pierson-Moskowitz spectrum is

$$S_{PM}(F^*) = \frac{5h_s^2 T_0}{16} \frac{1}{(F^*)^5} \exp\left[-\frac{5}{4}(F^*)^{-4}\right] \quad (1)$$

In Eq. (1), h_s is the significant wave height, T_0 is the dominant wave period, and F^* is the ratio of wave frequency to the dominant wave frequency. In a linear system, it can be characterized in the frequency domain by an expression of the form:

$$Y(f) = H(f)X(f) \quad (2)$$

where f is the frequency, $X(f)$ is the Fourier transform of the excitation, $Y(f)$ is the Fourier transform of the response, and $H(f)$ is the transfer function. For offshore structures, the excitation is the elevation of the sea's surface, the response is the hot spot stress ranges (HSSR) at the joins, and the transfer function is the hot spot stress range value for waves with unit amplitude. The RMS (Root-Mean-Square) value of the cyclic stress range for a particular point of joint and sea state is

$$\sigma_{RMS_i} = \sqrt{\int_0^\infty H^2(f)S_i(f)df} \quad (3)$$

where $S_i(f)$ is the spectral density and $H(f)$ is the transfer function for the direction being considered. The zero-crossing period for every RMS stress (σ_{RMS}) is given by:

$$T_z = \frac{\sigma_{RMS_i}}{\sqrt{\int_0^\infty f^2 H^2(f)S_i(f)df}} \quad (4)$$

The number of cycles related to a given sea state with the probability of occurrence, m , during the lifetime of the structure, L , is equal to

$$n(s) = \frac{mL}{T_z} \quad (5)$$

Cumulative fatigue damage, according to Palmgren-Miner's (1945) rule, is obtained from Eq. (6). This rule represents that for the different cases of waves, the total damage is equal to the summation of induced damage from each wave.

$$D = \frac{n(s)}{\sigma_{RMS_i}^2} \int_0^\infty \frac{s}{N(s)} \exp\left(-\frac{s^2}{2\sigma_{RMS_i}^2}\right) ds \quad (6)$$

The stress range in Eq. (6) is denoted by "s" while "N(s)" represents the maximum number of cycles allowed within that range, obtained from the S-N curve of API RP 2A (2007).

4. Numerical modeling

In this paper, four platforms with heights of 70, 90, 120, and 150 meters (Fig. 3) are modeled and analyzed using OpenSees software. The geometric characteristics of these four platforms are presented in Table 2. Braces and legs are modeled by the Nonlinear-beam-column element. This element can accept non-linear behavior and the possibility of considering the formation of a plastic hinge along the length of the element. The modulus of elasticity, yield stress, and Poisson's ratio of the material are considered equal to 200 GPa, 340 MPa, and 0.3, respectively. Because the purpose of this paper was to investigate the effects of local joint flexibility and stress range changes in joints, pile-soil-structure effects were not considered, and a pile stub with a length of 10D (D is the pile diameter) was modeled at the end of each leg. The application of regular waves and calculation of forces were performed using Airy wave theory and Morrison's equation, respectively.

5. Analysis results of sample platforms

5.1 Modal analysis results

The frequency content of the structure is important in cyclic excitation, and this becomes more significant when the excitation period is close to the natural period of the structure. In addition, the time step for dynamic analysis is determined based on the modal analysis results (The time step for force is chosen to be less than 1/20 of the structure's first natural period and the wave period). As a result, it is necessary to investigate the effects of considering local joint flexibility on the periods of the structure. The natural periods of the first eight modes of the sample platforms are depicted in Fig. 4. The analysis of this figure indicates a significant impact of the LJF on the results of modal analysis. For example, when Jacket (A) is modeled with rigid joints, the first mode period is 2.023 seconds. However, considering the inclusion of local joint flexibility, the first mode period for Jacket (A) increases by 2.67% and 23.08% using the equivalent element and flexible link approaches, respectively. Fig. 4 also demonstrates the high sensitivity of the second mode of the structure to the joint modeling technique. Employing the flexible link approach results in an average 92.85% higher period for the second mode across the four sample platforms than the period obtained from the rigid link approach. Due to the direct consideration of the joint geometry in the stiffness matrix, the flexible link approach has resulted in more alterations in the frequency content of the structure. For example, the inclusion of flexibility using the equivalent element approach led to an average increase

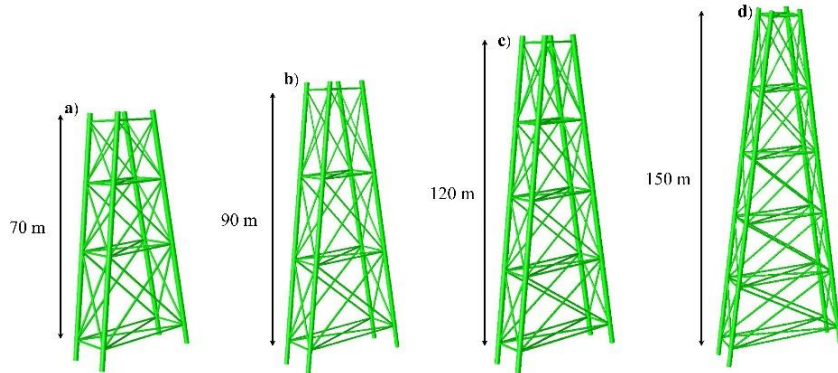


Fig. 3 Four platforms with a height of 70 (a), 90 (b), 120 (c), and 150 (d) meters have been modeled and analyzed

Table 2 The geometric characters of the four studied platforms

	Jacket (A)	Jacket (B)	Jacket (C)	Jacket (D)
Leg	1700x20 mm	1700x20 mm	2200x20 mm	2200x20 mm
Pile	1600x67 mm	1600x67 mm	2100x67 mm	2100x67 mm
Brace in level 1	700x20 mm	700x20 mm	800x20 mm	900x20 mm
Brace in level 2	600x20 mm	600x20 mm	700x20 mm	800x20 mm
Brace in level 3	500x20 mm	500x20 mm	700x20 mm	700x20 mm
Brace in level 4	-	-	700x20 mm	700x20 mm
Brace in level 5	-	-	-	700x20 mm
Horizontal brace	600x20 mm	600x20 mm	700x20 mm	800x20 mm

of 2.95% in the periods of Jacket (C). However, when flexibility was considered using the flexible link approach, the structure's period increased by 39.6%.

5.2 Fatigue analysis results

In this section, the results of fatigue analysis are presented for the tubular joints of sample platforms, which are labeled as shown in Fig. 5. The first stage involved applying waves with a unit amplitude and a frequency range of 0.1 to 0.8 Hz (in increments of 0.05) to the structure. Dynamic analysis was performed to obtain the axial and bending nominal stresses in all of the joints, which were then used to calculate the hot spot stresses by applying stress concentration factors. The HSSR was determined as the difference between the maximum and minimum hot spot stresses at various phase angles of the wave. This step resulted in generating a transfer function that describes the relationship between HSSR and wave frequency. The transfer functions for specific joints in Jacket (A) to (D) are illustrated in Figs. 6 to 9. Because the stress concentration factors are higher on the chord side than on the brace side, the transfer functions for the brace side are not presented. Section 5.1 showed that considering LJF can change the structure's frequency content and force distribution. Therefore, LJF should also affect the transfer functions.

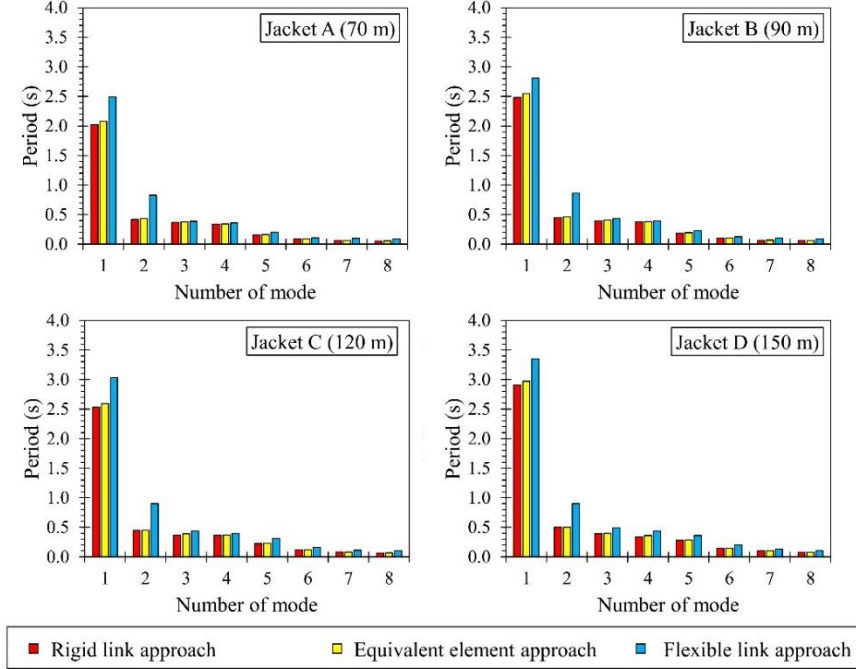


Fig. 4 Effect of LJF on the period of the first eight modes of the structure

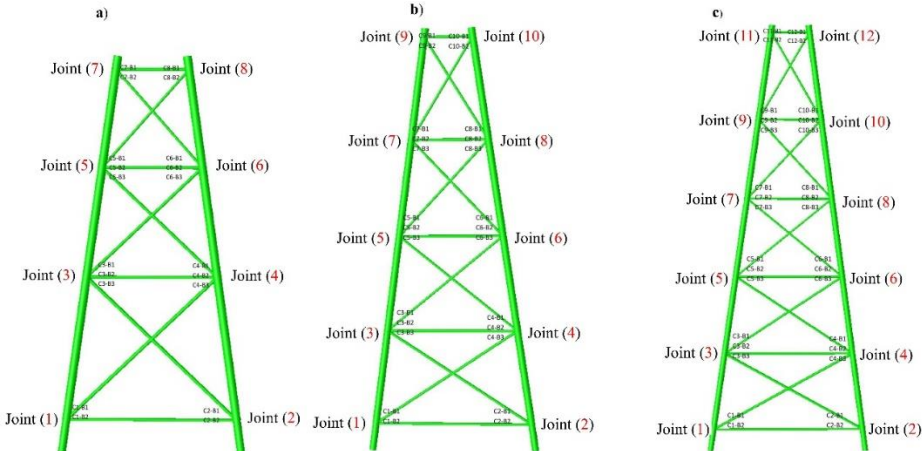


Fig. 5 The naming of joints in sample platforms

According to Fig. 6 to Fig. 9, the peak and dominant frequency of the transfer functions have significant changes depending on the joint modeling approach. For example, the rigid link approach shows that Joint (7) has a maximum transfer function value of 220.03 MPa in Jacket (A). However, when the equivalent element approach is employed to model the joints, the maximum transfer function value for Joint (7) in Jacket (A) decreases by 30.43%. The flexible link approach, which

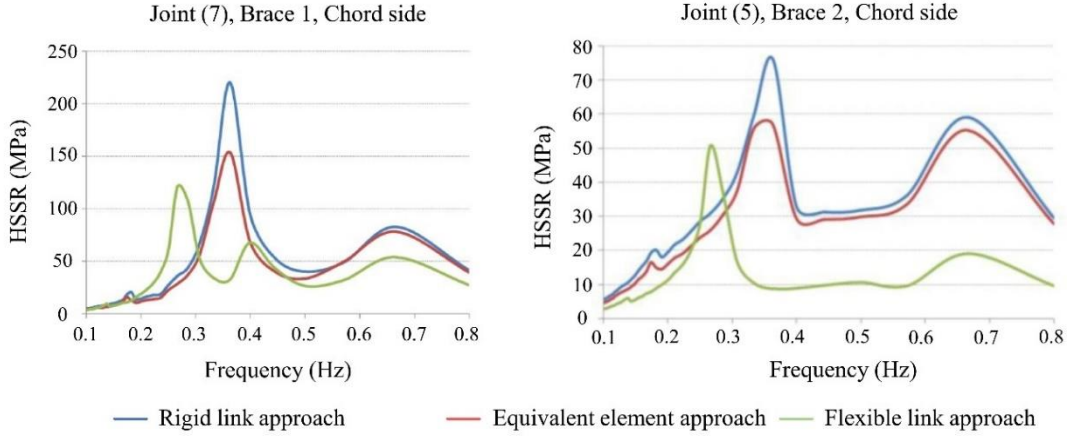


Fig. 6 The transfer functions for Joint (5) and (7) of Jacket (A)

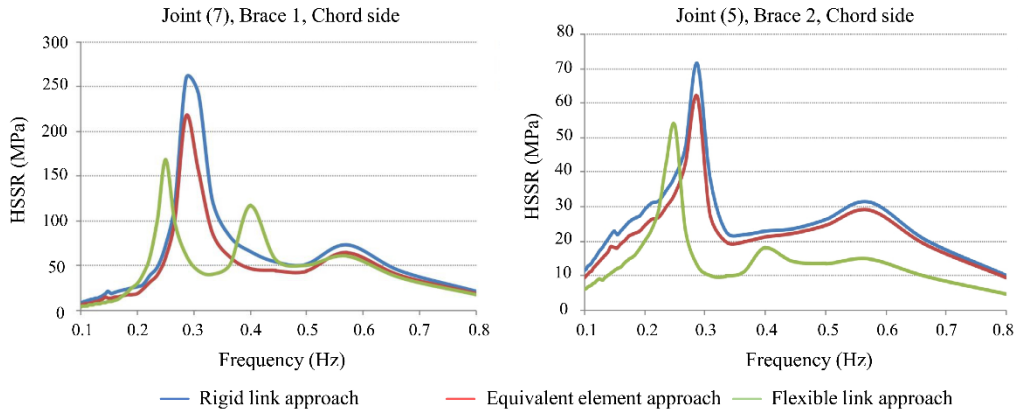


Fig. 7 The transfer functions for Joint (5) and (7) of Jacket (B)

directly incorporates joint geometry into the stiffness matrix, exerts a more significant impact on the maximum transfer function value for Joint (7). As depicted in Fig. 6, this approach yields a 44.35% reduction in the maximum transfer function value for Jacket (A) compared to the rigid link approach. The dominant frequency of the transfer function for Joint (5), as depicted in Fig. 6, is 0.3600 Hz. Although the equivalent element approach had a negligible impact on the dominant frequency, the flexible link approach resulted in a significant decrease of 25.71% in the dominant frequency.

Based on the scatter diagram for each sea state, induced damage is calculated, and by using a safety factor of two, the total damage is obtained. Predicted fatigue damage for Jacket (C) and (D) are presented in Tables 3 and 4. In these tables for different joints of jackets, total induced damage is presented. Tables 3 and 4 demonstrate that considering LJF influences cumulative fatigue damage. For example, in Joint (11) on the chord side at braces 1 and 2, Jacket (D) has fatigue damage equal to 1.1352 and 7.5324, respectively, according to the rigid link approach. However, using the equivalent element approach to model this joint reduced fatigue damage by 75.79% and 39.35%

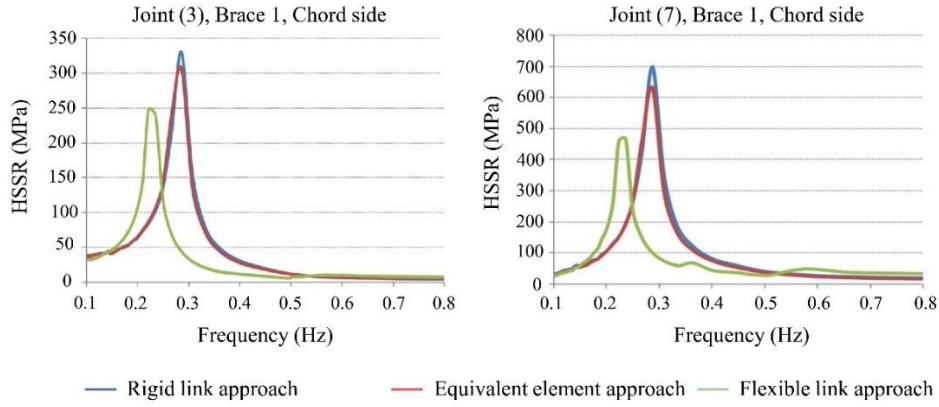


Fig. 8 The transfer functions for Joint (3) and (7) of Jacket (C)

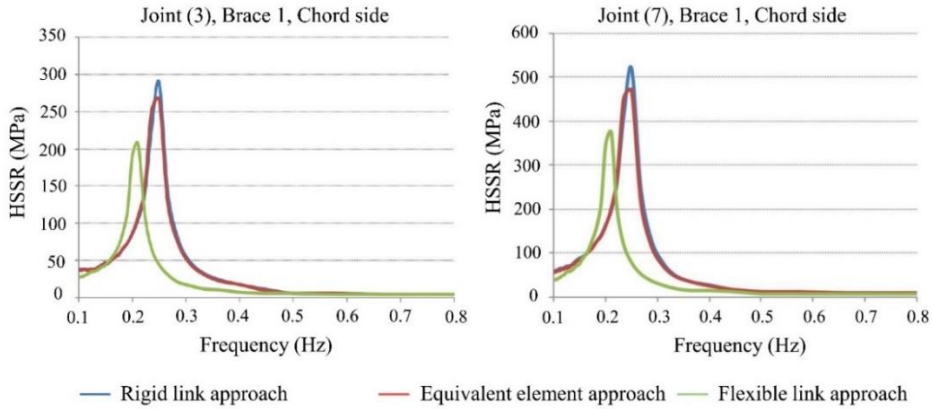


Fig. 9 The transfer functions for Joint (3) and (7) of Jacket (D)

at braces 1 and 2, respectively, compared to the rigid link approach. The flexible link approach had an even more significant impact, as it increased the global flexibility of the structure, resulting in increased displacement and decreased inertia force of the member. Modeling Joint (11) using the flexible link approach reduced fatigue damage by 97.69% and 95.64% at braces 1 and 2, respectively, compared to the rigid link approach.

As the height of the jacket increases, the effect of LJF on fatigue damage is more noticeable. Because with the increase in the structure's height, the mass participation of the higher modes will increase in the dynamic response of the structure. In Joint (9) of Jacket (C), modeling the joint by the flexible link approach has led to an 88.06% reduction in fatigue damage compared to the rigid link approach at brace 2. However, the modeling of Joint (11) of Jacket (D), which has a more elevated height than Jacket (C), by flexible link approach has led to a 95.64% reduction in fatigue damage compared to the rigid link approach at brace 2.

The occurrence rates for inducing failure ($D_{\text{Fatigue}} = 1.0$) in Joint (7) of Jacket (A) are presented in Tables 5 and 6. These tables illustrate that the inclusion of LJF results in an increase in the

Table 3 Total induced damage in the connections of Jacket (C)

Joint Name	Joint modeling approach	Brace 1		Brace 2		Brace 3	
		Brace	Chord	Brace	Chord	Brace	Chord
Joint (9)	Rigid link	0.0489	0.1632	2.0560	5.9160	-	-
	Equivalent element	0.0238	0.0583	1.4066	3.6270	-	-
	Flexible link	0.0170	0.0242	0.2764	0.7063	-	-
Joint (7)	Rigid link	0.0501	0.5188	0.0084	0.0133	0.1430	0.4989
	Equivalent element	0.0421	0.4009	0.0065	0.0119	0.1203	0.4029
	Flexible link	0.0137	0.0636	0.0000	0.0000	0.0229	0.0768
Joint (5)	Rigid link	0.0190	0.0930	0.0000	0.0003	0.0570	0.1503
	Equivalent element	0.0171	0.0801	0.0000	0.0001	0.0501	0.1297
	Flexible link	0.0037	0.0157	0.0000	0.0000	0.0093	0.0244
Joint (3)	Rigid link	0.0105	0.0367	0.0000	0.0000	0.0093	0.0173
	Equivalent element	0.0099	0.0324	0.0000	0.0000	0.0086	0.0153
	Flexible link	0.0019	0.0057	0.0000	0.0000	0.0018	0.0033

Table 4 Total induced damage in the connections of Jacket (D)

Joint Name	Joint modeling approach	Brace 1		Brace 2		Brace 3	
		Brace	Chord	Brace	Chord	Brace	Chord
Joint (11)	Rigid link	0.2452	1.1352	2.6178	7.5324	-	-
	Equivalent element	0.0687	0.2748	1.7631	4.5683	-	-
	Flexible link	0.0164	0.0262	0.1294	0.3280	-	-
Joint (9)	Rigid link	0.0345	0.3432	0.0108	0.0163	0.1124	0.3744
	Equivalent element	0.0323	0.3126	0.0093	0.0143	0.1018	0.3366
	Flexible link	0.0044	0.0305	0.0000	0.0005	0.0079	0.0272
Joint (7)	Rigid link	0.0171	0.0816	0.0003	0.0012	0.0327	0.0799
	Equivalent element	0.0157	0.0732	0.0001	0.0008	0.0307	0.0745
	Flexible link	0.0018	0.0063	0.0000	0.0000	0.0033	0.0073
Joint (5)	Rigid link	0.0073	0.0264	0.0000	0.0001	0.0264	0.0568
	Equivalent element	0.0066	0.0240	0.0000	0.0000	0.0247	0.0529
	Flexible link	0.0013	0.0026	0.0000	0.0000	0.0025	0.0048
Joint (3)	Rigid link	0.0042	0.0143	0.0000	0.0000	0.0017	0.0031
	Equivalent element	0.0038	0.0130	0.0000	0.0000	0.0017	0.0028
	Flexible link	0.0012	0.0015	0.0000	0.0000	0.0008	0.0012

occurrence rate for failure. For example, in the first sea state, the required occurrence rate for failure in the second brace of Joint (7) is equal to 71.855 (on the brace side) in the rigid modeling mode. However, when Ljf is considered in the equivalent element and flexible link approaches, the occurrence rates become 17.01 and 62.10 times higher than the rigid modeling mode, respectively. Thus, considering Ljf leads to an increase in the joint's fatigue life.

Table 5 Occurrence rates for inducing failure ($D_{\text{Fatigue}} = 1.0$) in Joint (7) of Jacket (A): A comparison between rigid modeling of joints and the equivalent element approach

Sea state	Brace 1				Brace 2			
	Brace side		Chord side		Brace side		Chord side	
	Rigid link	Equivalent element						
1	9632.3	17701.5	373.2	620.2	71.9	1222.6	27.6	84.2
2	24.78	25.01	23.12	23.41	18.35	24.56	7.15	19.43
3	18.80	19.61	10.82	12.41	4.82	14.75	1.19	5.43
4	91.46	375.28	43.85	65.45	19.27	23.48	10.16	13.44
5	26.96	34.68	9.88	21.43	0.40	0.53	0.18	0.25
6	6.33	14.37	1.59	4.33	0.06	0.08	0.03	0.04
7	158.15	1091.08	52.33	95.95	22.55	24.79	12.50	14.39
8	34.85	41.24	14.57	28.97	0.49	0.56	0.23	0.27
9	10.00	21.85	2.47	6.65	0.07	0.08	0.03	0.04
10	44.02	48.17	33.41	42.65	1.63	1.79	0.77	0.87
11	26.89	39.17	8.54	19.79	0.24	0.27	0.12	0.13
12	10.41	22.57	2.55	6.75	0.07	0.08	0.03	0.04
13	52.61	85.66	44.66	48.17	5.27	5.67	2.55	2.81
14	42.29	45.61	23.58	38.19	0.80	0.86	0.38	0.42
15	27.03	39.85	8.46	19.62	0.23	0.25	0.11	0.12
16	47.26	55.83	39.98	46.21	2.29	2.46	1.10	1.20
17	41.90	46.19	21.31	36.71	0.66	0.70	0.31	0.34
18	29.87	41.97	9.83	22.06	0.26	0.28	0.12	0.13

Table 7 displays the occurrence rates for inducing failure in Joint (11) of Jacket (D). By comparing this table with Table 6; it can be concluded that as the height of the structure increases, the importance of considering LJF becomes more evident. This observation becomes apparent when examining Jacket (A) with a height of 90 meters. In this case, the required occurrence rate for failure when utilizing the flexible link approach is, on average, 6.77 times higher compared to the required occurrence rate for failure in the case of rigid joint modeling. Meanwhile, for Jacket (D) with a height of 150 meters, the required occurrence rate for failure when employing the flexible link approach is, on average, 38.29 times higher than the required occurrence rate for failure in the case of rigid joint modeling.

6. Conclusions

In this paper, the effect of local joint flexibility (LJF) on the fatigue damage of tubular joints in jacket-type offshore platforms was investigated. To explore the impact of LJF on the fatigue damage of tubular joints, the paper employed three different approaches for modeling flexibility: rigid link (without LJF), equivalent element, and flexible link. Modal and spectral fatigue analysis was conducted on sample platforms in OpenSees software to compare the effectiveness of these approaches. The following observations can be made:

Table 6 Occurrence rates for inducing failure ($D_{\text{Fatigue}} = 1.0$) in Joint (7) of Jacket (A): A comparison between rigid modeling of joints and the flexible link approach

Sea state	Brace 1				Brace 2			
	Brace side		Chord side		Brace side		Chord side	
	Rigid link	Flexible link						
1	9632.3	Infinite	373.2	Infinite	71.9	75926.7	27.6	597.0
2	24.78	40.79	23.12	28.31	18.35	26.39	7.15	23.38
3	18.80	24.20	10.82	22.67	4.82	21.43	1.19	12.29
4	91.46	Infinite	43.85	1740.49	19.27	54.19	10.16	47.50
5	26.96	39.01	9.88	36.38	0.40	13.59	0.18	6.32
6	6.33	31.69	1.59	21.70	0.06	2.23	0.03	0.97
7	158.15	2831.02	52.33	169.43	22.55	37.25	12.50	21.88
8	34.85	49.07	14.57	40.29	0.49	0.96	0.23	0.43
9	10.00	30.22	2.47	11.06	0.07	0.14	0.03	0.06
10	44.02	55.36	33.41	49.58	1.63	1.35	0.77	0.61
11	26.89	42.18	8.54	18.04	0.24	0.20	0.12	0.09
12	10.41	20.06	2.55	5.74	0.07	0.06	0.03	0.03
13	52.61	71.09	44.66	56.51	5.27	3.40	2.55	1.54
14	42.29	53.52	23.58	36.19	0.80	0.51	0.38	0.23
15	27.03	38.76	8.46	14.46	0.23	0.14	0.11	0.07
16	47.26	58.68	39.98	52.41	2.29	1.35	1.10	0.61
17	41.90	52.96	21.31	31.48	0.66	0.38	0.31	0.17
18	29.87	40.55	9.83	15.37	0.26	0.15	0.12	0.07

- The paper's findings suggest that considering local joint flexibility (LJF) in the analysis of the studied platforms led to notable changes in the frequency content of the structure. In particular, the period of the first mode of the structure increased by up to 23.08% when LJF was considered. This indicates that the flexibility of the joints influences the platform's dynamic behavior. When LJF is considered, the second mode of the structure is more affected by the joint modeling approach. In particular, the LJF simulation with the flexible link approach resulted in a period increase of up to 100% for the second mode.
- Due to the reduction in the dominant frequency by considering LJF, a 44.35% decrease in the maximum value of the transfer function is observed.
- The flexible link approach is the most reliable way to model the LJF. By considering joint geometry in the stiffness matrix, this approach yields a longer joint fatigue life than the equivalent element approach, making it the preferable choice for accurate fatigue analysis.
- The impact of LJF on fatigue damage becomes more pronounced as a jacket-type offshore platform increases in height. This is due to the increased mass participation of higher modes in the structure's dynamic response. Therefore, it is crucial to consider the effects of flexibility on taller offshore platforms to ensure accurate fatigue analysis.
- LJF reduces joint fatigue damage because the transfer function is altered by LJF.
- Including LJF in the modeling of platform joints leads to an increase in the occurrence rate for induced failure ($D_{\text{Fatigue}} = 1.0$), which can be up to 62.10 times higher than in rigid joint modeling.

Table 7 Occurrence rates for inducing failure ($D_{\text{Fatigue}} = 1.0$) in Joint (11) of Jacket (D): A comparison between rigid modeling of joints and the flexible link approach

Sea state	Brace 1				Brace 2			
	Brace side		Chord side		Brace side		Chord side	
	Rigid link	Equivalent element						
1	480.261	Infinite	61.147	Infinite	4014.9	Infinite	72.045	29998.43
2	23.66	45.608	17.42	29.228	24.836	35.566	18.569	25.902
3	11.765	24.707	4.215	23.141	17.517	24.137	4.841	20.682
4	46.302	1067.813	40.818	153.395	47.291	165.861	38.596	65.978
5	10.839	37.405	2.684	31.87	4.11	34.328	1.389	21.66
6	1.757	20.154	0.402	9.446	0.619	10.195	0.206	4.222
7	24.68	159.961	5.872	66.642	3.19	39.099	1.183	18.491
8	0.494	41.42	0.099	17.469	0.053	0.907	0.019	0.336
9	0.073	10.764	0.015	2.904	0.008	0.134	0.003	0.05
10	0.409	21.655	0.081	5.182	0.038	0.127	0.014	0.047
11	0.061	3.611	0.012	0.778	0.006	0.019	0.002	0.007
12	0.017	1.034	0.003	0.221	0.002	0.005	0.001	0.002
13	0.856	25.176	0.169	5.956	0.075	0.131	0.028	0.049
14	0.127	4.276	0.025	0.896	0.011	0.019	0.004	0.007
15	0.036	1.226	0.007	0.255	0.003	0.006	0.001	0.002
16	0.312	8.003	0.062	1.684	0.026	0.035	0.01	0.013
17	0.089	2.323	0.018	0.479	0.007	0.01	0.003	0.004
18	0.035	0.91	0.007	0.187	0.003	0.004	0.001	0.002

Consequently, incorporating LJF in fatigue analysis is crucial for obtaining reliable and cost-effective assessments of offshore platforms. It offers a more accurate representation of the platform's behavior under cyclic loading, leading to improved structural reliability, safety, and performance. Additionally, LJF-aware fatigue analysis can inform design enhancements, maintenance planning, and inspection strategies, providing long-term benefits for both new and existing jacket-type offshore platforms.

Acknowledgments

The authors gratefully acknowledge the useful comments of anonymous reviewers on the draft version of this paper.

References

- Abdel Raheem, S.E., Abdel Aal, E.M., AbdelShafy, A.G., Fahmy, M.F. and Mansour, M.H. (2022), "In-place analysis for pile structural response of fixed jacket offshore platform", *Ship Offshore Struct.*, **17**(6), 1224-1237. <https://doi.org/10.1080/17445302.2021.1906039>

- Ahmadi, H. and Akhtegan, M. (2022), "Effects of geometrical parameters on the local joint flexibility (LJF) of three-planar tubular T-joints in offshore structures", *Ship Offshore Struct.*, **17**(7), 1604-1615. <https://doi.org/10.1080/17445302.2021.1937794>
- Ahmadi, H. and Janfeshan, N.M. (2021), "Local joint flexibility of multi-planar tubular TT-joints: Study of geometrical effects and the formulation for offshore design practice", *Appl. Ocean Res.*, **113**, 102758. <https://doi.org/10.1016/j.apor.2021.102758>
- Ahmadi, H. and Niri, A.A. (2023), "Geometrical effects on the local joint flexibility of three-planar tubular Y-joints in substructures of offshore wind turbines", *Ship Offshore Struct.*, 1-13. <https://doi.org/10.1080/17445302.2023.2179213>
- Alanjari, P., Asgarian, B. and Kia, M. (2011), "Nonlinear joint flexibility element for the modeling of jacket-type offshore platforms", *Appl. Ocean Res.*, **33**(2), 147-157. <https://doi.org/10.1016/j.apor.2010.12.005>.
- American Petroleum Institute (API) (2007), Recommended practice for planning, designing and constructing fixed offshore platforms: Working stress design: RP 2A-WSD. 21nd Edition, Errata and Supplement 3, Washington DC, US.
- Asgarian, B., Alanjari, P. and Aghaeidoost, V. (2015), "Three-dimensional joint flexibility element for modeling of tubular offshore connections", *J. Mar. Sci. Tech.*, **20**, 629-639. <https://doi.org/10.1007/s00773-015-0317-2>
- Buitrago, J., Healy, B.E. and Chang, T.Y. (1993), "Local joint flexibility of tubular joints", *Proceedings of the International Conference on Ocean, Offshore & Arctic Engineering (OMAE)*, Glasgow, 405-417. <https://trid.trb.org/view/444857>.
- Gao, F., Hu, B. and Zhu, H.P. (2013), "Parametric equations to predict LJF of completely overlapped tubular joints under lap brace axial loading", *J. Constr. Steel Res.*, **89**, 284-292. <https://doi.org/10.1016/j.jcsr.2013.07.010>.
- Golafshani, A.A., Kia, M. and Alanjari, P. (2013), "Local joint flexibility element for offshore platforms structures", *Mar. Struct.*, **33**, 56-70. <https://doi.org/10.1016/j.marstruc.2013.04.003>.
- Han, C., Mo, C., Tao, L., Ma, Y. and Bai, X. (2022), "An efficient fatigue assessment model of offshore wind turbine using a half coupling analysis", *Ocean Eng.*, **263**, 112318. <https://doi.org/10.1080/17445302.2021.1906039>.
- Khan, R., Smith, K. and Kraincanic, I. (2018), "Improved LJF equations for the uni-planar gapped K-type tubular joints of ageing fixed steel offshore platforms", *J. Mar. Eng. Technol.*, **17**(3), 121-136. <https://doi.org/10.1080/20464177.2017.1299613>.
- Ladeira, I., Márquez, L., Echeverry, S., Le Sourne, H. and Rigo, P. (2022), "Review of methods to assess the structural response of offshore wind turbines subjected to ship impacts", *Ship Offshore Struct.*, **18**(6), 755-774. <https://doi.org/10.1080/17445302.2022.2072583>.
- Miner, M.A. (1945), "Cumulative damage in fatigue", *J. Appl. Mech.*, **12**(3), 159-164. <https://doi.org/10.1115/1.4009458>.
- Mirtaheri, M., Zakeri, H.A., Alanjari, P. and Assareh, M.A. (2009), "Effect of joint flexibility on overall behavior of jacket type offshore platforms", *Am. J. Eng. Appl. Sci.*, **2**(1), 25-30. <https://doi.org/10.3844/ajeassp.2009.25.30>.
- Nassiraei, H. and Rezadoost, P. (2022), "Stress concentration factors in tubular T-joints reinforced with external ring under in-plane bending moment", *Ocean Eng.*, **266**, 112551. <https://doi.org/10.1016/j.oceaneng.2022.112551>.
- Ren, C., Aoues, Y., Lemosse, D. and De Cursi, E.S. (2021), "Comparative study of load simulation approaches used for the dynamic analysis on an offshore wind turbine jacket with different modeling techniques", *Eng. Struct.*, **249**, 113308. <https://doi.org/10.1016/j.engstruct.2021.113308>.
- Ren, C., Aoues, Y., Lemosse, D. and De Cursi, E.S. (2023), "Reliability assessment of an offshore wind turbine jacket under one ultimate limit state considering stress concentration with active learning approaches", *Ocean Eng.*, **281**, 114657. <https://doi.org/10.1016/j.oceaneng.2023.114657>.
- Xu, T., Li, Y. and Leng, D. (2023), "Mitigating jacket offshore platform vibration under earthquake and ocean waves utilizing tuned inertial damper", *Bull. Earthq. Eng.*, **21**(3), 1627-1650. <https://doi.org/10.1007/s10518-022-01378-z>.

Zhu, H., Shao, Y., Chi, G., Gao, X. and Li, K. (2022), "Simplified bar-system model for tubular structures by considering local joint flexibility", *Mar. Struct.*, **81**, 103122. <https://doi.org/10.1016/j.marstruc.2021.103122>.

KA